Bioactive Materials 6 (2021) 1910–1920

Contents lists available at ScienceDirect

Bioactive Materials

journal homepage: www.sciencedirect.com/journal/bioactive-materials

Design of a biofluid-absorbing bioactive sandwich-structured Zn–Si bioceramic composite wound dressing for hair follicle regeneration and skin burn wound healing

Zhaowenbin Zhang [a,b,1], Wenbo Li [c,1], Ying Liu [d], Zhigang Yang [d], Lingling Ma [a,b], Hui Zhuang [a,b], Endian Wang [a,b], Chengtie Wu [a,b], Zhiguang Huan [a,b], Feng Guo [c,**], Jiang Chang [a,b,*]

[a] State Key Laboratory of High Performance Ceramics and Superfine Microstructure, Shanghai Institute of Ceramics, Chinese Academy of Sciences, 1295 Dingxi Road, Shanghai, 200050, People's Republic of China
[b] Center of Materials Science and Optoelectronics Engineering, University of Chinese Academy of Sciences, 19 Yuquan Road, Beijing, 100049, People's Republic of China
[c] Department of Plastic Surgery, Shanghai Jiaotong University Affiliated Sixth People's Hospital, Shanghai, PR China
[d] Plastic Surgery Hospital, Chinese Academy of Medical Sciences and Peking Union Medical College, Beijing, PR China

ARTICLE INFO

Keywords:
Burn wound healing
Hair follicle regeneration
Zn^{2+} and SiO_3^{2-}
Sandwich-structured wound dressing
Janus membrane)

ABSTRACT

The deep burn skin injures usually severely damage the dermis with the loss of hair follicle loss, which are difficult to regenerate. Furthermore, severe burns often accompanied with large amount of wound exudates making the wound moist, easily infected, and difficult to heal. Therefore, it is of great clinical significance to develop wound dressings to remove wound exudates and promote hair follicle regeneration. In this study, a sandwich-structured wound dressing (SWD) with Janus membrane property was fabricated by hot compression molding using hydrophilic zinc silicate bioceramics (Hardystonite, ZnCS) and hydrophobic polylactic acid (PLA). This unique organic/inorganic Janus membrane structure revealed excellent exudate absorption property and effectively created a dry wound environment. Meanwhile, the incorporation of ZnCS bioceramic particles endowed the dressing with the bioactivity to promote hair follicle regeneration and wound healing through the release of Zn^{2+} and SiO_3^{2-} ions, and this bioactivity of the wound dressing is mainly attributed to the synergistic effect of Zn^{2+} and SiO_3^{2-} to promote the recruitment, viability, and differentiation of hair follicle cells. Our study demonstrates that the utilization of the Janus membrane and synergistic effect of different type bioactive ions are effective approaches for the design of wound dressings for burn wound healing.

1. Introduction

Hair follicle, residing in the dermal layer of the skin, is one of the main appendages of the skin. The hair follicle stem cells locating in the bulge of the outer root sheath of the hair follicle can differentiate into the epidermis and contribute to re-epithelialization in the process of skin wound healing [1,2]. However, when the skin is deeply burned, the epidermis and dermis are damaged and the hair follicle tissue under the dermis disappears, which is difficult to regenerate [3]. The loss of the hair follicle tissue will reduce the rate of skin re-epithelialization, and significantly affects the original beauty and functionality of the skin [2,4,5]. At the same time, severe burns often accompanied with large amount of wound exudates, which may hinder the healing process and easy to cause infection [6–8]. Previous studies on skin burn wound dressings (such as colloid gel, nanomaterials and so on) often focus on antibacterial, anti-inflammatory functions of the material and the enhancement of skin healing process [9,10], while the regeneration of functional skin appendages such as hair follicles is less investigated and

Peer review under responsibility of KeAi Communications Co., Ltd.
* Corresponding author. State Key Laboratory of High Performance Ceramics and Superfine Microstructure, Shanghai Institute of Ceramics, Chinese Academy of Sciences, 1295 Dingxi Road, Shanghai, 200050, People's Republic of China.
** Corresponding author.
E-mail addresses: guofengburn@aliyun.com (F. Guo), jchang@mail.sic.ac.cn (J. Chang).
[1] These authors contributed equally to this work.

https://doi.org/10.1016/j.bioactmat.2020.12.006
Received 31 August 2020; Received in revised form 9 December 2020; Accepted 9 December 2020

no wound dressings with dual-functions of unidirectional wound exudate absorption and hair follicle growth promotion are reported [11–13]. Therefore, it has clinical significance to develop wound dressings for solving these two problems.

In recent years, natural algae have become one of the most popular active substances in the beauty cosmeceuticals industry due to their excellent potential to enhance skin vitality and activate hair follicle tissue [14,15]. Natural algae are a type of aquatic single-celled organisms, mainly composed of various algae organisms such as diatoms, cyanobacteria, and red algae. Previous studies have shown that algae extracts have the effect of wound healing and stimulating the activity of hair follicles [16–18]. It is interesting to see through literature analysis that algae extracts contain many trace elements including abundant Zn and Si [19–21].

Zn is an indispensable trace element in the growth of hair follicles. It is an essential cofactor for more than 300 enzymes, such as alkaline phosphatase [22,23], dopachrome tautomerase [24], metallothionein [25], and metalloproteinase [26], which play important functional activities in hair follicles. It can be found that Zn^{2+} is inseparable from the state of hair follicles in the human body [27,28]. For example, when treating androgenetic alopecia, proper zinc intake can significantly prolong the regression of hair follicles caused by spontaneous apoptosis [27,29], and in a recent study, we demonstrated that wound dressings containing zinc have activity to promote the growth of hair follicle tissue [30]. In addition, silicate bioceramics have been found to have bioactivity by releasing silicate ions, which activate specific gene expression related to skin healing, stimulate endothelial cell proliferation and migration, and promote vascularization during tissue regeneration [31–35]. At the same time, many studies have confirmed that different ions may have a special synergistic effect, and this synergistic effect may further promote tissue regeneration and wound healing [36–39]. Inspired by the composition of natural algae extracts and related function, one of our hypotheses is that Zn^{2+} and SiO_3^{2-} may have specific synergistic effect on hair follicle regeneration during burn wound healing.

Many silicate bioceramics have been found to release multiple ions with different bioactivities to stimulate tissue regeneration [40–42]. In addition, dry ceramic powders in general have certain capacity to absorb water, and when applied to a wound bed with exudates, they may result in the removal of wound exudates and create a dry wound environment for better healing. However, due to the irregular and sharp shape of the ceramic particles, direct application of bioceramic powders to the wound may result in adhesion of the ceramic particles to the surface of the wound. Moreover, wound fluids may also cause the loss of ceramic particles, which may affect treatment effect [38].

A Janus membrane with hydrophobic property on one side and hydrophilic on the other side has the function to transport fluids from the hydrophobic side to the hydrophilic side, which makes it possible to remove exudates from wound bed [8]. Traditional Janus membranes are in general consist of two type of polymer layers with different hydrophilicity/hydrophobility. We know that most of silicate bioceramic powders are hydrophilic. Therefore, we assume that if a silicate

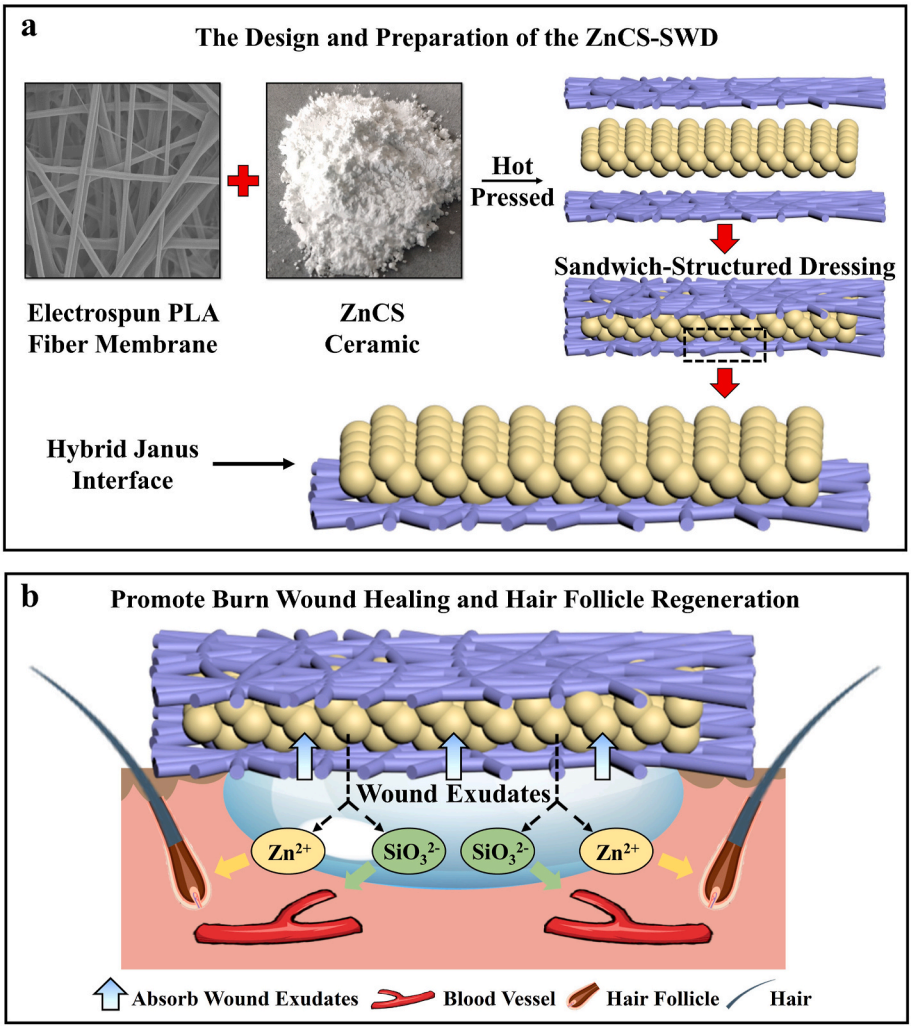

Fig. 1. A biofluid absorbing sandwich-structured wound dressing (SWD) designed by organic-inorganic hybrid Janus membrane containing hardystonite (ZnCS, $Ca_2ZnSi_2O_7$) and the application in deep burn wound healing with enhanced hair growth and angiogenesis. (The wound fluid is absorbed by the powder in the sandwich dressing, which then releases bioactive ions for stimulating the regeneration of blood vessels and hair follicles.) (a) The design and preparation of the ZnCS-SWD. (b) ZnCS-SWD promote burn wound healing and hair follicle regeneration.

bioceramic particle layer combined with a hydrophobic polymer fibrous membrane, the formed hybrid interface may has the function of Janus interface, and may be able to absorb wound exudates from wound bed without direct contact of the ceramic powders with the wound bed, while the ceramic powders can release Zn^{2+} and SiO_3^{2-} ions once they are in contact with the wound fluids. With this consideration, we designed a sandwich-structured wound dressing using a hydrophobic polymer fiber membrane (PLA) wrapped with hydrophilic zinc-containing silicate bioceramics (Hardystonite, ZnCS) (Fig. 1). This structure can absorb the wound exudates to create a dry and clean wound surface [8]. Meanwhile, the dressing has the activity to promote hair follicle regeneration and wound healing through the release of Zn^{2+} and SiO_3^{2-} active ions, and also avoid the possible damage to the wound caused by direct contact of sharp ceramic particles with the wound. The effectiveness of this ZnCS containing sandwich-structured wound dressing (ZnCS-SWD) was investigated by a third-degree scald mouse model, and the synergistic activity and related mechanisms of Zn^{2+} and SiO_3^{2-} in stimulating hair follicle regeneration was studied through in vitro cell experiments.

2. Material and methods

2.1. Characterization of the sandwich-structured wound dressing (SWD)

First, PLA was dissolved in hexafluoroisopropanol (10%, w/v) and stirred for 24 h. Then, a fiber membrane was prepared by electrospinning using the above prepared solution. The flow rate was 0.02 mL/min, and the voltage was 12 kV. The collection distance between the tip and the rotating collector was fixed at 15 cm. The electrospun fiber membranes were collected after 4 h electrospinning. The prepared PLA fiber membrane was placed in a vacuum drying oven (30 °C) for 48 h to remove residual organic solution [43]. The SWD composite dressings were prepared by combining two pieces of PLA fiber membranes with hardystonite bioceramic powders. The PLA fiber membrane was cut into a suitable size (1*1 cm^2–2*2 cm^2) and the bioceramic powders (CS, ZnCS, 0.5 g/cm^2) of appropriate quality were added on one piece of PLA fiber membranes and then covered with another piece of PLA membrane. Thereafter, the material was sealed by a sealing machine, and then the sealed package was hot pressed (80 °C, 30Mpa) by a hot-pressing machine (R-3201, Wuhan QiEn Science & Technology Development Co., Ltd., China).

Thereafter, the surface morphology of the SWD was observed through a scanning electron microscope (SEM, S-4800, Hitachi, Japan). The size distribution of the ZnCS powders was analyzed using a laser particle size analyzer (Bettersize2600, Bettersize Instruments LTD, China). The hydrophilic property of the SWD was studied by video contact angle meter (SL200B, Shanghai Solon Information Technology Co., Ltd.). The water absorption property of the material was evaluated by weighing. Finally, the materials (1*1 cm^2) were soaked in 10 mL phosphate buffered saline (PBS) for 24h, and the ion release of the materials were measured by ICP-AES (Thermo Fisher X Series 2, USA).

2.2. Establishment of a burn animal model

8-week-old Sprague Dawley (SD) rats were purchased from CAS Shanghai Laboratory Animal Center (SLACAS). All animal operations were performed in accordance with the guidelines for the care and use of laboratory animals in Shanghai Jiao Tong University (Shanghai, China), and approved by the Animal Ethics Committee of the Sixth People's Hospital Affiliated to Shanghai Jiao Tong University School of Medicine (Shanghai, China). A total of 30 rats were used in this study and lived in the Laboratory Animal Center of the Sixth People's Hospital of Shanghai Jiao Tong University School of Medicine in a pathogen-free environment. In order to test the actual application ability of SWD prepared by ZnCS powder (ZnCS-SWD), we modified the previous scheme [44] to prepare a full-thickness third-degree burn wound model. A total of 30 rats were randomly divided into 3 groups with 10 for each group. A custom metal iron bar ($\Phi = 20$ mm) was boiled in hot water at 100 °C for more than 10 min. It was pressed on the back of the rat for 15s to cause a third-degree burn wound (average area size, 450 mm^2). Each wound was created with a single application of the preheated metal iron bar, and two wounds were created on the back of each rat. The wound was disinfected with 75% alcohol for 10 s after the burn. Next, different wound dressing packages (ZnCS and CS) were sutured on the wound with surgical sutures and further bandaged with 3 M wound dressing, and PLA dressing was used as a negative control group (Blank). Change the wound dressing on days 3, 10, and 17. Burned animals were fed in cages and checked daily.

2.3. Wound healing rate

Photographs of the wound area were taken on days 0, 3, 10, 17, and 24 post operation, and scale stickers were used as a size reference. The size of the wound area at different time points was determined by Photoshop CS 6.0. The wound healing rate was calculated as the percentage of the healed wound area relative to the original burn wound area.

2.4. Histological analysis

Tissue samples were obtained on days 10 and 24 post operation and fixed in 4% paraformaldehyde for 48 h. After paraffin embedding, the tissue samples were cut into 7 μm sections and processed according to our previous work [45]. Briefly, the sections were stained using hematoxylin and eosin (H&E, Sigma-Aldrich) for histological analysis according to the manufacturer's instructions. For immunostaining, the sections were blocked with 10% goat serum in PBS for 1 h at room temperature. The primary antibody solution containing cytokeratin 19 (sc-376126, Santa Cruz, 1:400), rabbit anti-CD31 (ab9498, Abcam, 1:200), or rabbit anti-collagen I (ab34719, Abcam, 1:100) was diluted to the appropriate ratio with PBS and used to incubate the samples at room temperature for 2 h. Then, biotinylated goat anti-rabbit IgG (orb153693, Biorbit, 1:500) was diluted to the appropriate ratio with PBS and used as a secondary antibody to incubate the samples at room temperature for 1 h. After labeling, the staining was visualized using DAB staining followed by hematoxylin counterstaining. The tissue specimens were examined by microscopy for the analysis of angiogenesis, collagen deposition, epithelialization, and hair follicle formation. The number of new hair follicles on day 24 was determined by counting six random selected image areas according to the cytokeratin 19 staining. The number of new blood vessels on days 10 and 24 was counted, and the diameter of new blood vessels on day 24 was determined by randomly counting three areas according to the CD31 staining using ImageJ program.

2.5. Preparation of calcium silicate (CS) and hardystonite (ZnCS) bioceramic ion extracts

CS and ZnCS powders (more than 400 mesh) were purchased from Kunshan Huaqiao Technology New Materials Co., Ltd. According to ISO/EN 10993-12, a series of gradient-diluted ion extracts of CS and ZnCS powders were prepared. Firstly, CS or ZnCS powders were added into serum-free Mesenchymal Stem Cell Medium (MSCM, Gibco) and William's E medium (Gibco) at a solid/liquid ratio of 200 mg/mL. The mixture was centrifuged at 4000 rpm for 10 min after being incubated at 37 °C for 24 h. Then the supernatant was sterilized by filtration through 0.22 μm filter membranes and collected to obtain stock solutions. Subsequently, the stock solution was diluted with serum-free MSCM and William's E medium to prepare the gradient diluted ion extracts (1/4, 1/8, 1/16, 1/32, 1/64, 1/128 dilutions), and all the ion extracts were stored at 4 °C for further investigating the effects of different concentrations of ion extracts.

2.6. Cell culture

Human hair follicle dermal papilla cells (HHDPCs) were cultured in Mesenchymal Stem Cell Medium (MSCM) containing 5% (vol/vol) fetal bovine serum (FBS, Thermo Trace Ltd, Melbourne, Australia) and 1% (vol/vol) mesenchymal stem cell growth supplements (MSCGS). In this study, all cells used were between the 5th and 7th passages.

2.7. The effect of ion products from ZnCS on HHDPCs

2.7.1. Cell viability and proliferation

In order to evaluate the viability of HHDPCs in media containing different ZnCS ion products, HHDPCs were seeded into 96-well plates at a density of 1×10^3 cells per well and cultured with MSCM medium. After incubation for 24 h, the culture medium was replaced by 100 μL of serial ZnCS diluted ion extracts (1/4, 1/8, 1/16, 1/32, 1/64, 1/128). HHDPCs cultured with MSCM were used as a blank control group (Blank), and the cells cultured with CS extracts and Zinc chloride solution were used as control groups. Then, the cells were constantly cultured for 5 days, and a Cell Counting Kit (CCK)-8 assay (Beyotime) was applied on cells at 1, 3 and 5 days according to the manufacturer's instruction. Briefly, the culture medium was removed and replaced with fresh medium containing CCK-8 (10:1), and the cells were further cultured at 37 °C in an incubator for 2 h at the end of each culture time point. The absorbance of the reaction product was measured using an enzyme-linked immunoabsorbent assay microplate reader (Synergy 2, Bio-TEK) at a wavelength of 450 nm. The results were shown as units of optical density (OD) absorbance value, which represented the metabolic activity of cells.

In order to evaluate the effect of Zn^{2+} and SiO_3^{2-} on HHDPCs proliferation activity, HHDPCs were seeded into 6-well plates at a density of 1×10^5 cells per well and cultured with MSCM medium. After incubation for 24 h, the culture medium was replaced by 2 mL of 1/16 ZnCS ion extracts and cultured for 5 days. Then, cells were treated with 2.5% Trypsin, and the cell number was counted using the Neubauer chamber. HHDPCs cultured with MSCM were used as a blank control group (Blank), and the cells cultured with CS extracts and Zinc chloride solution were used as control groups.

Finally, the proliferation rate and viability rate of the cells were calculated using following formulas:

$$\text{Cell proliferation rate} = \text{Ce/Cb*100\%}$$

$$\text{Cell viability rate} = \text{ODe/ODb*100\%}$$

Where Ce is the cell number of experimental groups (Zn, ZnCS, CS), and Cb is the cell number of the Blank group, Ode is the OD value of experimental groups (Zn, ZnCS, CS), and ODb is the OD value of the Blank group.

2.7.2. In vitro HHDPCs migration

The assay was conducted according to a published method [33] to evaluate the effect of Zn^{2+} and SiO_3^{2-} on HHDPCs cellular migration activity. First, cells were seeded in a 6-well plate and cultured up about 80% confluent, followed by serum-free starvation over 24 h to reset the cell cycle. Then, the cell monolayer in each well was scrapped with a plastic tip (200 μL) and washed with PBS (0 h). Then, the cell culture medium was replaced with 0.5% serum 1/16 ZnCS ion extract, 0.5% serum MSCM were used as a blank control group (Blank), and the same concentration of CS extract and zinc chloride solution served as a control group. Thereafter, optical images were obtained at 0 and 12 h by using an optical microscope (Leica). After 12 h, the cells were stained with crystal violet (CV) for 1 min, and optical images were obtained using the above optical microscope. The migration rate was analyzed by Image J software and determined by the ratio of the initial scratch area and the final scratch area.

2.7.3. Hair follicle differentiation related gene expression

Gene expression of VEGF, BMP-6, HGF, KGF, PDGF-α, PDGF-β, and C-Myc in HHDPCs were detected by Q-RT-PCR [46–49]. HHDPCs were plated in 6-well plates at a density of 1×10^5 cells/well for 24h. Then, the culture medium was removed, and 1/16 ZnCS ion extracts were applied to cells (MSCM were used as a blank control group, and the same concentration of CS extract and zinc chloride solution served as a control group). After incubation for 72 h, HHDPCs were slightly washed twice with preheated PBS and total RNA was extracted from cells using Trizol reagent (Invitrogen). The concentrations of total RNA were assayed by a nanodrop 2000 reader (Thermo Scientific). Then, cDNA was synthesized using a Prime-Script™ RT reagent kit (Takara Bio, Shiga, Japan) according to manufacturer's recommendations. Primers for the stem cell markers containing VEGF, BMP-6, HGF, KGF, PDGF-α, PDGF-β, C-Myc and the housekeeping gene GAPDH were synthesized commercially (Shengong, Co. Ltd. Shanghai, China). Quantification of all cDNA of stemness marker genes was performed with Bio-Rad MyiQ single color Real-time PCR system. All experiments were done in triplicate to obtain the average data. The sequences of primers were as follows: VEGF (5′-GCG AGT CTG TGT TTT TGC AG-3′ and 5′-TCT TCA AGC CAT CCT GCG TG-3′), BMP-6 (5′-AAC CAA CCA CGC GAT TGT G-3′ and 5′-AAG TCT CAT CGT CCC ACC TC-3′), HGF (5′-ACA CCA GGG TGA TTC AGA CC-3′ and 5′-CGA GGC CAT GGT GCT ATA CT-3′), KGF (5′-AAT TCC AAC TGC CAC TGT CC-3′ and 5′-GAC ATG GAT CCT GCC AAC TT-3′), PDGF-α (5′-GAA TCA TAG CTC TCT CCT CGC AC-3′ and 5′-GAT TCC TCC AAA GCC TCA TAG CAG-3′), PDGF-β (5′-CAG TCC TGC CTG TCC TTC TAC TC-3′ and 5′-GGA TCT GGC ACA AAG ATG TAG AGC-3′), C-Myc (5′-AAT AGA GCT GCT TCG CCT AGA-3′ and 5′-GAG GTG GTT CAT ACT GAG CAA G-3′) and GAPDH (5′-TGG CAA ATT CCA TGC AC-3′ and 5′-CCA TGG TGG TGA AGA CGC-3′).

2.7.4. Human hair follicles culture

Human hair follicles were obtained from the Plastic Surgery Hospital (Institute) of the Chinese Academy of Medical Sciences, which were isolated and cultured following a method described previously [50]. Isolated human hair follicles were cut from the bottom of the dermal papillary and cultured in William's E medium (Gibco) containing diluted ZnCS E culture medium extracts (1/16 dilution) and supplemented with 10 ng/mL hydrocortisone, 10 μg/mL insulin, 2 mM L-glutamine, and 1 × antibiotic/antimycotic solution at 37 °C in a 5% CO_2 atmosphere. The normal Williams E culture medium was used as a blank control group, and the William's E medium containing CS extract or zinc chloride in same concentration as that in ZnCS group also served as control groups (n = 6). Thereafter, the hair follicles were observed and the length were measured at different time points up to 12 days using a stereomicroscope (Olympus).

2.8. Statistical analysis

All results were expressed as means ± standard deviation. Multiple comparisons between groups were performed using one-way ANOVA testing with a post hoc test. Statistical significance was considered when $^*P < 0.05$, $^{**}P < 0.01$ or $^{***}P < 0.001$.

3. Results

3.1. The characterization of the ZnCS sandwich-structured wound dressing (ZnCS-SWD)

The ZnCS-SWDs in different size were prepared by using polylactic acid (PLA) fiber membrane and ZnCS bioceramic powder by hot pressing (Fig. 2a). Under the optical microscope, we can clearly observe that the PLA fiber membrane and the ZnCS powder constitute a three-layer structure (Fig. S1). The SEM observation of the inside and outside of the PLA fiber membrane in SWD showed that ZnCS particles adhere to the inner side fibers, while few particles adhere to the outer surface of

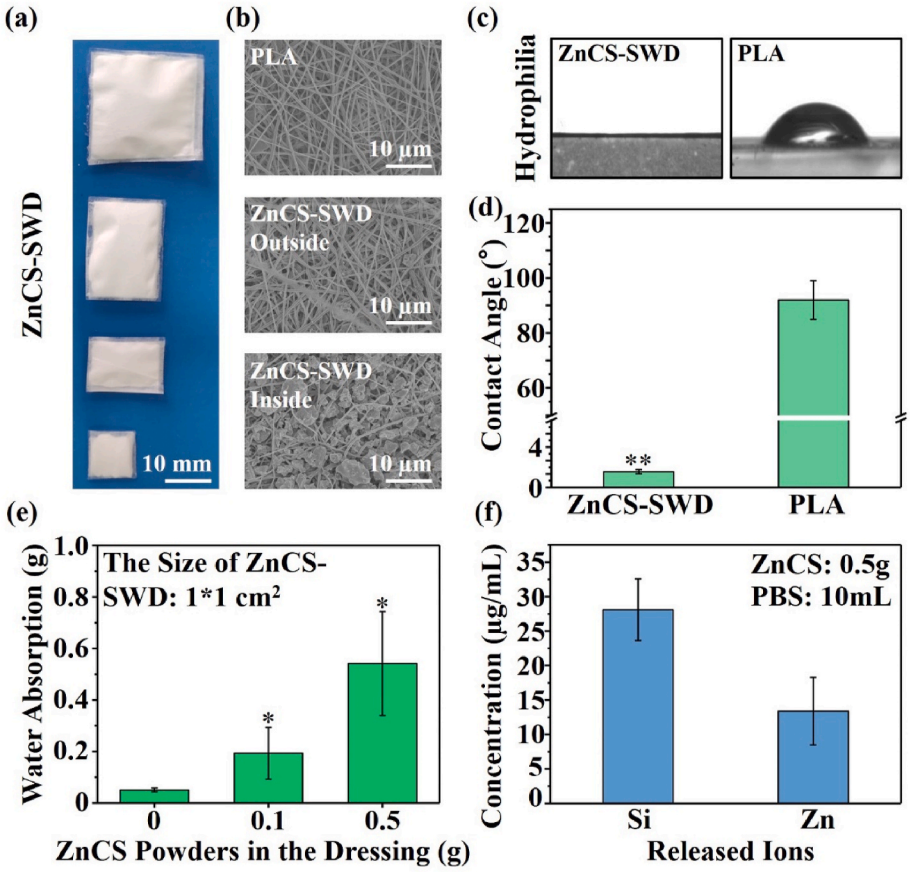

Fig. 2. Material characterization of ZnCS sandwich-structured wound dressing (ZnCS-SWD) (PLA fiber membrane was used for comparison). (a) The macroscopic appearance of the ZnCS-SWD. (b) The SEM of the ZnCS-SWD (Outside: the side not in contact with the ceramic powders; Inside: the side directly in contact with the ceramic powders). (c) Photos of the water contact angle of the ZnCS-SWD surface. (d) Quantitation of the contact angle of the ZnCS-SWD. (e) The water absorption performance of the ZnCS-SWD (1*1 cm^2) with different amount of bioceramic powders. (f) The ion release of the ZnCS-SWD (1*1 cm^2) by soaking in PBS at 37 °C for 24 h.

the fibers (Fig. 2b). Since the average particle size of the ceramic powder is about 2.548 μm (Fig. S2) similar as the inter-fiber distance, particles can be easily embedded between interwoven fibers (Fig. 2b). With this design, a hydrophilic/hydrophobic interface is formed between the hydrophobic organic polymer layer and the hydrophilic inorganic ceramic powder layer. This Janus interface endows the dressing with the ability to transport fluids in one direction [8]. It can be found from the contact angle results that the PLA fiber membrane alone is 91.96 ± 7.06°, while the ZnCS-SWD is 2.34 ± 0.32° (Fig. 2c and d). And the absorption amount of the ZnCS-SWD increased with the increase of the ZnCS powder content in the dressing (Fig. 2e). Movie S1 also shows that the single-layer PLA fiber membrane has little ability to absorb water, while the double-layer structure of PLA and ZnCS bioceramic powder can quickly absorb liquid, and the liquid quickly penetrates the ZnCS bioceramic powder layer. Furthermore, in the three-layer structure of ZnCS-SWD, we found that although the liquid is quickly absorbed, it does not penetrate the PLA layer on the other side. The liquid was stored in the ceramic powder in the middle layer. Furthermore, after soaking the ZnCS-SWD in PBS, Zn^{2+} and SiO_3^{2-} were detected indicating good ion release property of the dressing (Fig. 2f). The concentration of the released SiO_3^{2-} is 28.11 ± 4.48 ppm, and that of the Zn^{2+} is 13.40 ± 4.89 ppm after 1day soaking, which are in the bioactive concentration range for regulating cellular behavior [45].

Supplementary data related to this article can be found at https://doi.org/10.1016/j.bioactmat.2020.12.006.

3.2. Effect of ZnCS-SWD on hair follicle regeneration and wound healing in vivo

3.2.1. Wound appearance and closure

To evaluate the effects of ZnCS-SWD on wound healing and hair follicle regeneration in burn wound, a third-degree scald model was used (Fig. 3a) (SWD prepared using calcium silicate without Zn (CS-SWD) and PLA dressing was used as control groups.) [44,51]. Fig. 3b shows a macro image of the wound. It can be found that from the 0^{th} day to 3rd day, scald wounds of each group formed and gradually became larger. On the 10th day, the wounds treated with ZnCS-SWD did not have obvious scabs, while the Blank group and the CS-SWD group developed thick scabs. On the 17th day, the wounds treated with ZnCS-SWD contracted and quickly healed, and a small amount of hair tissue was observed around the wounds. In the CS-SWD group, the scab on the wound began to come off, and the wound gradually healed. However, the wound area of the Blank group was not significantly reduced, and a large amount of tissue fluid was observed. On the 24th day, the wounds treated with the ZnCS-SWD group were almost completely closed, and the surrounding hair follicles grew further inward. The scabs in the CS-SWD group continued to fall off, and the wounds were further reduced. However, there was still tissue fluid in the Blank group, accompanied by a slight infection, and the wound had not yet healed. In addition, on the 24th day, no obvious hair follicle was observed in the Blank and the CS-SWD groups. The quantitative analysis confirmed that ZnCS-SWD group exhibited a faster wound healing rate compared with the Blank and CS-SWD groups on the 17th, and 24th day (Fig. 3c).

3.2.2. Histological and immunohistochemical analysis

Burns can cause long-term sustained damage to skin tissue. H&E staining (Fig. 3d) showed that on the 10th day, all the hair follicle tissue originally retained in the dermis disappeared, and the cells in the dermis layer were largely apoptotic, forming many holes in each group. However, compared with the Blank and CS-SWD groups, the ZnCS-SWD group began to form a new dermal layer, and the cavity in the dermal layer became smaller with time. On the 24th day, the dermal layer in the ZnCS-SWD group is almost completely healed, and a new epidermal

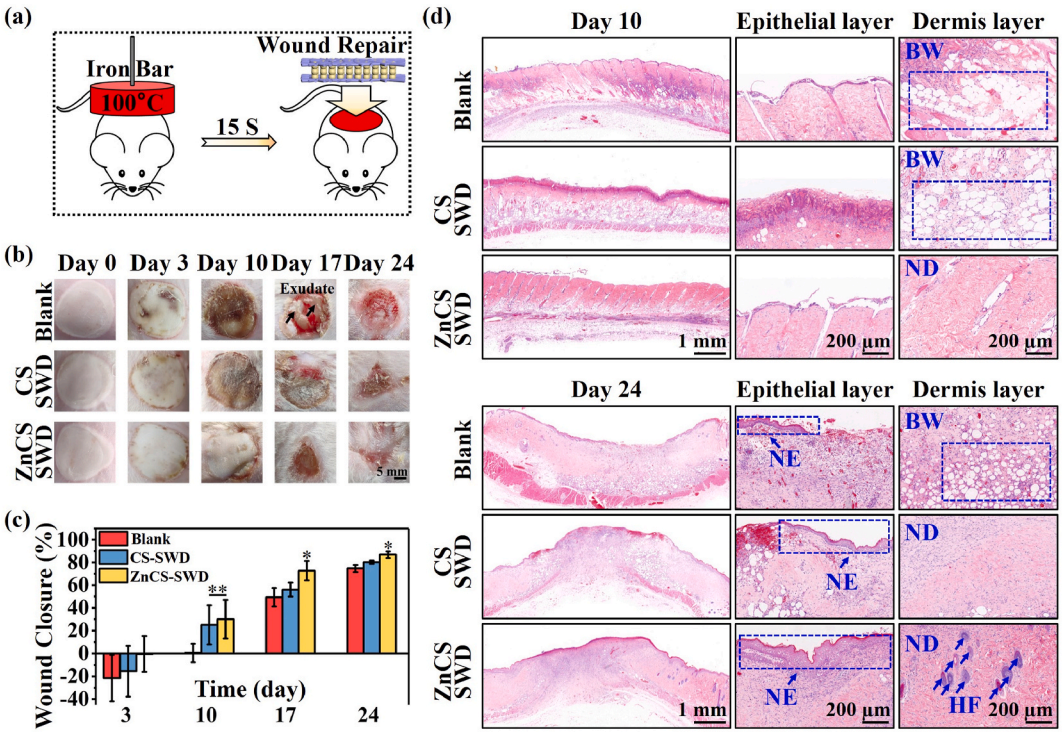

Fig. 3. (a) Establishment of a burn animal model using a hot metal iron bar and use sandwich-structured wound dressing for treatment. (b) Wound closure after treatment with sandwich-structured wound dressing. Wound area images on the 0^{th}, 3rd, 10th, 17th, and 24th day after treatment with different materials (blank was treated with PLA dressings). (c) Quantitation of wound closure rate of composite membranes (n = 4). (d) Images of H&E staining of wound sections on the 10th and 24th day (BW: Burn wound; NE, newly formed epidermis; ND, newly formed dermis; HF, newly formed hair follicle). *P < 0.05 and **P < 0.01.

layer has been formed. In addition, new hair follicle tissue was also observed. In contrast, in the Blank and CS-SWD groups, the dermal layer still had some defects, the epidermal layer was almost invisible, and hardly any hair follicle tissue was observed.

The regeneration of hair follicles in wounds was further observed by immunohistochemical staining of hair follicle stem cell marker K19 (Fig. 4a). On the 10th day, after treatment with ZnCS-SWD, the recruitment of hair follicle stem cells at the wound site was clearly observed, and a small amount of hair follicle precursor tissues could be found. In contrast, the skin tissues in the Blank and CS-SWD groups were still in the repairing stage, and no hair follicle-related cells were observed. On the 24th day, many gradually mature hair follicles appeared in the ZnCS-SWD group. As compared with the ZnCS-SWD group, K19 staining with lower intensity was also found in the CS-SWD group, indicating that the hair follicle-related cells began to aggregate and immature hair follicle tissues started to appear. In contrast, no K19 positive staining was observed in the Blank group. In addition, the number of hair follicles of ZnCS-SWD group on the 24th day was also significantly higher than that of the CS-SWD group, while hardly any hair follicle was observed in the Blank group (Fig. 4b). Furthermore, we have counted the hair follicle number at the edge of burn wound on 10th day and 24th day. The results are shown in Fig. S3. It is clear to see that the wound closure of Blank group on day 24 is comparable with that of the ZnCS-SWD group at day 10 (Fig. S3a), while the hair follicle number of ZnCS-SWD group at day 10 is significantly higher than that of the Blank group at day 24 (Fig. S3b). This result suggest that the ZnCS-SWD group promotes hair follicle regeneration as compared with the Blank group.

Vascularization of the wound area is an important part of wound healing and provides sufficient nutrition during wound healing. Fig. 4c shows the immunohistochemical staining of CD31, which is a marker of endothelial cells. The results showed that on the 10th and 24th days, more CD31 positive staining was clearly observed in the wound areas treated by the ZnCS-SWD and CS-SWD groups, while less CD31 positive staining was found in the Blank group. The quantitative analysis confirmed that the ZnCS-SWD group had the highest neovascularization on the 10th and 24th days. At the same time, some new blood vessels also appeared in the CS-SWD group. In contrast, only a small amount of new blood vessels appeared in the Blank group (Fig. 4d). In addition, it is interesting that on 24th day, ZnCS-SWD produced more blood vessels with larger diameters (Fig. 4e).

Collagen synthesis of fibroblasts in the dermis also plays an important role in wound healing. Fig. S4 shows the collagen I deposition at different time periods. It can be clearly seen that in the early stage of the 10th day, the amount of collagen deposition in the ZnCS-SWD group was significantly higher than that in the Blank and CS-SWD groups, which indicated that ZnCS-SWD were beneficial to stimulate the early collagen secretion. On the 24th day, the amount of collagen deposition in the ZnCS-SWD group gradually weakened as compared with the 10th day, proving that the wound had almost completely healed [52].

3.3. Synergistic effects of Zn^{2+} and SiO_3^{2-} (ZnCS) on the migration, viability, proliferation, and gene expression of hair follicle dermal papilla cells (HHDPCs) in vitro

In order to further investigate the synergistic effect between Zn^{2+} and SiO_3^{2-}, a separate Zn^{2+} solution (Zn), a separate SiO_3^{2-} solution (CS), and a Zn^{2+}/SiO_3^{2-} mixed solution with same Zn^{2+} and SiO_3^{2-} concentrations (ZnCS) were used to culture HHDPCs. For cell migration, it was found that both Zn^{2+} (71.24 ± 1.31%) and SiO_3^{2-} (68.09 ± 4.82%) ions alone effectively promoted HHDPCs migration, and the ZnCS further enhanced cell migration, indicating a synergistic effect of Zn^{2+} and SiO_3^{2-}. (Fig. 5a and b). However, we found that only Zn^{2+} enhanced the viability and proliferation of HHDPCs cells, while SiO_3^{2-} did not show obvious activity to enhance cell viability and proliferation. More interestingly, the ZnCS significantly promoted cell viability and proliferation as compared with Zn^{2+} alone, indicating that the combination of Zn^{2+} and SiO_3^{2-} has a significant synergistic active effect in enhancing cell

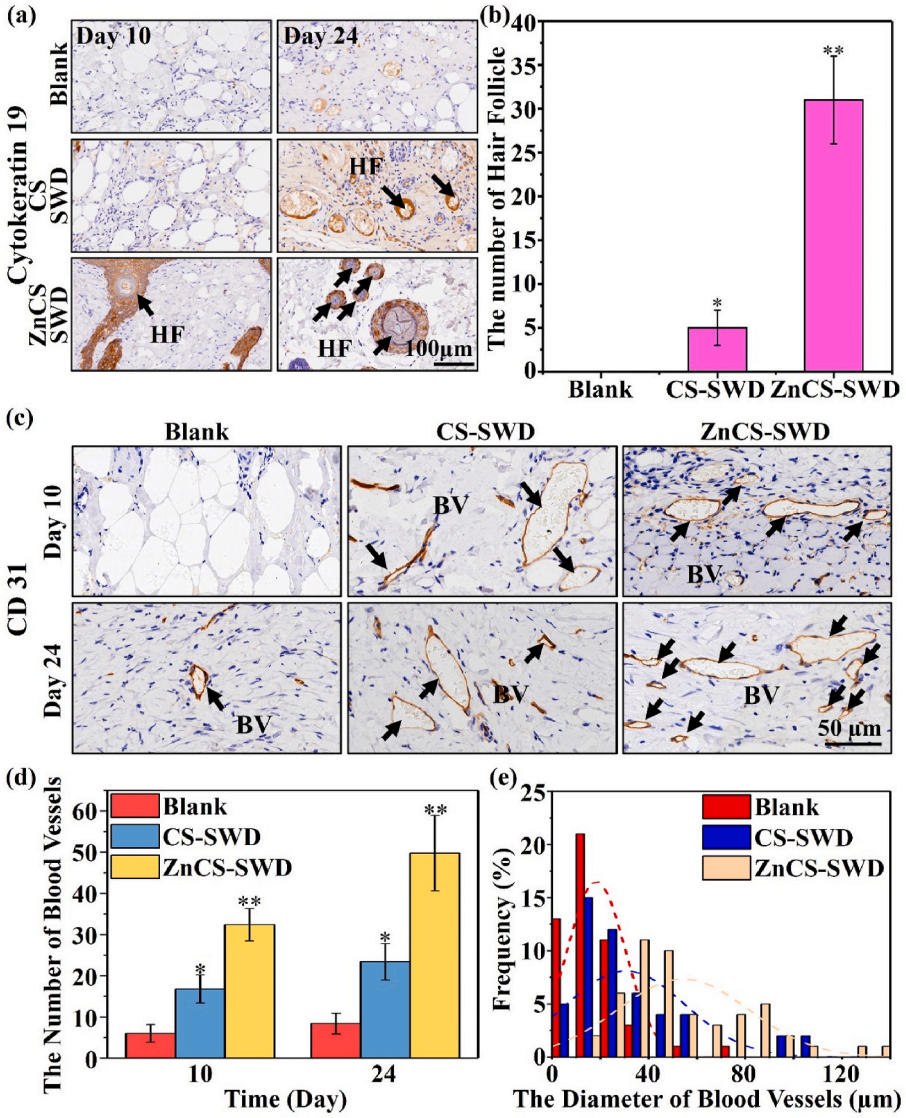

Fig. 4. (a) Images of immunohistochemical staining for cytokeratin 19 on the 10th and 24th day (HF, newly formed hair follicles). (b) Number of hair follicles on the 24th day (n = 6). (c) Images of immunohistochemical staining for CD31 on the 10th and 24th day (BV, blood vessels). (d) Number of blood vessels on the 10th and 24th day. (e) Vessel diameter distribution on the 24th day. (*P < 0.05, **P < 0.01, n = 3).

viability and proliferation (Fig.5c and Fig. S7). Furthermore, we have compared the cell numbers with the results of CCK8 analysis on the 5th day (Fig. S7, Table S1). It can be found that in different groups, there is no significant difference between the number of cells and the results of CCK8. This proves that our material mainly stimulates cell proliferation. In addition, a clear synergistic effect of the Zn^{2+}/SiO_3^{2-} combination in stimulating expression of growth factors (Stem cell indicator markers: VEGF, BMP-6, KGF, HGF; Hair follicle anagen markers: PDGF-α, PDGF-β, and C-Myc) was observed [46–49]. For stem cell indicator markers, Zn^{2+} alone only revealed limited enhancement of the expression of VEGF and BMP-6, but not HGF and KGF, while SiO_3^{2-} alone did not show any stimulation effect on the expression of growth factors of HHDPCs. For hair follicle anagen markers, both Zn^{2+} and SiO_3^{2-} could stimulate the expression of PDGF-α, and C-Myc, but not PDGF-β. In contrast, the combination of Zn^{2+}/SiO_3^{2-} showed significant stimulation effect on the expression of all these genes indicating the stimulation of hair follicle growth (Fig. 5d).

3.4. Synergistic effects of Zn^{2+} and SiO_3^{2-} (ZnCS) on human hair follicle growth in ex vivo culture

In order to further observe the influence of the synergistic effect of Zn^{2+} and SiO_3^{2-} on the hair follicles growth, a separate Zn^{2+} solution (Zn), a separate SiO_3^{2-} solution (CS), and a Zn^{2+}/SiO_3^{2-} mixed solution with same Zn^{2+} and SiO_3^{2-} concentrations (ZnCS) were used to culture human hair follicles. The results showed that the hair follicles cultured with ZnCS were significantly longer than that non-treated and treated only with Zn or with CS after the 6 days, while no significant difference was observed between the Zn and CS and Blank groups (Fig. S8a). It is noticed that in the Zn and Blank groups hair follicles longer maintained the original shape and the top of the hair follicles began to shrink significantly after 12 days of culture indicating the start of the degeneration phase of the cultured hair follicles. In contrast, the original morphology of the hair follicles in the ZnCS and CS groups were still maintained in the growth phase (Fig. S8b).

4. Discussion

In recent years, natural algae have become one of the most popular

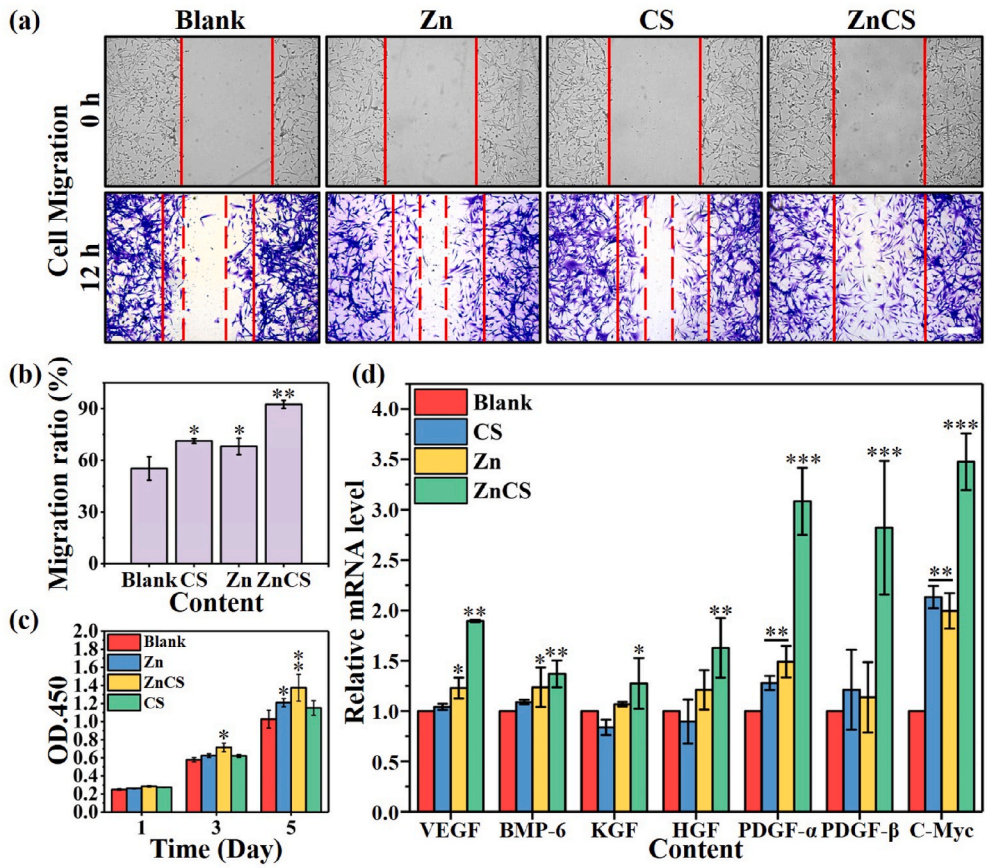

Fig. 5. Synergistic effect of Zn and Si ions on the migration, viability and gene expression of hair follicle dermal papilla cells (HHDPCs) (1/16 ZnCS extracts were used as Zn and Si ions solution. CS extracts (CS) and Zinc chloride solution (Zn) with same concentration were used as control groups). (a) The synergistic effect of Zn and Si ions on the migration of HHDPCs cells (Ruler Length = 200 μm). (b) Migration rate of HHDPCs. (c) The synergistic effect of Zn and Si ions on the viability of HHDPCs. (d) The synergistic effect of Zn and Si ions on genes (VEGF, BMP-6, KGF, HGF, PDGF-α, PDGF-β, and C-Myc) related to the hair follicle growth in HHDPCs (*P < 0.05, **P < 0.01, ***P < 0.001).

active substances in the beauty cosmeceuticals industry due to their excellent potential to enhance skin vitality and activate hair follicle tissue [14,15]. By analyzing the composition of algae reported in literatures, we found that it contains silicon and many trace elements including Zn [19–21]. Interestingly, some recent studies found that Zn^{2+} have activity to stimulate hair follicles regeneration and silicate ions are able to stimulate skin wound healing [30,38]. Therefore, we assume that the bioactive effect of algae on activation of hair and skin may closely related to the combination effect of these two types of ions. Considering the problems of hair follicle regeneration [44] and wound exudates removal [6–8], which are two critical issues for burn wound healing, we propose the following two hypotheses. First, Zn^{2+} and SiO_3^{2-} may have synergistic effect on hair follicles regeneration during wound healing. Second, a hydrophilic ceramic particle layer combined with a hydrophobic polymer fiber membrane layer may form a Janus interface with unidirectional liquid transportation ability for effective removal of wound exudates from wound bed. To confirm our hypotheses, we used zinc silicate bioceramics (Hardystonite, ZnCS) as hydrophilic Zn^{2+} containing silicate bioceramic particle layer and electrospun polylactic acid (PLA) as hydrophobic polymer layer to prepare a sandwich-structured wound dressing. It is confirmed that such a structure indeed formed a Janus membrane with unidirectional fluid transportation ability, and the composite dressing released Zn^{2+} and SiO_3^{2-}. At the same time, its ability to promote burn wound healing and hair follicle regeneration during the healing process was verified in a rat burn experimental model.

One of the factors hindering the wound healing of severe burns is large amounts of wound exudates, and effective removal of the exudates and creation of a dry environment in wound bed is critical for the burn healing process [6–8]. Traditional Janus membranes are constructed with one type of polymer material containing hydrophilic surface on one side and hydrophobic surface on the other side and less inorganic Janus membranes are reported. In this study, we for the first time constructed an organic-inorganic hybrid Janus membrane using a hydrophobic organic polymer (PLA) and hydrophilic Zn-containing silicate bioceramic (hardystonite) powders for wound exudates removal by hot pressing ceramic powders with PLA fibrous sheets. And due to the pressure and higher temperature, ceramic powders formed a ceramic particle layer with small amounts of ceramic particles penetrated into the fibrous polymer layer. Therefore, the hydrophilic ceramic layer is well integrated with the hydrophobic PLA to form a Janus interface, which has the function to unidirectionally transport fluid from polymer side to ceramic side. Our results demonstrate that the interface formed by the combination of a fibrous polymer layer and a ceramic particle layer indeed has unidirectional liquid transport property (Movie.S1) due to the unique hydrophobic and hydrophilic properties on different side of the membrane. The embedding of ceramic particles in fibrous layer of the polymer membrane resulted in the change of hydrophobicity to hydrophilicity on this side of the membrane (Fig. 2b, c and 2d). Based on this finding, we designed a sandwich-structured wound dressing with one ceramic powder layer wrapped in two fibrous polymer layers. With this design, the bottom layer hydrophobic PLA fiber membrane prevents the hydrophilic bioceramic powder from sticking directly to the wound and damaging the wound surface (Fig. S9), while the wound exudates are able to effectively transport from wound bed to the dressing due to the Janus membrane characteristics created by the combination of the hydrophobic PLA layer and ceramic powder layer. In the third-degree rat burn animal model, we observed that, in both the ZnCS-SWD and CS-SWD groups, as long as the composite dressings were applied, no exudate was appeared on the wound surface (Fig. 3b), which confirmed the effective unidirectional exudates removal capacity of the composite dressing.

Hair follicle regeneration is one of the challenges in burn wound healing, and one of the important finding of the present study is the

enhancement of hair follicle formation in third-degree burn model by the treatment of Zn–Si containing ZnCS-SWD composite wound dressing. In order to understand the reason why the ZnCS-SWD dressing has biological activity to promote hair follicle regeneration, we investigated the synergistic activity of Zn^{2+} and SiO_3^{2-} on hair follicle dermal papilla cells (HHDPCs). Interestingly, we found that both Zn^{2+} and SiO_3^{2-} can enhance the migration of HHDPCs (Fig. 3b and d), while cell viability is mainly affected by Zn^{2+} (Fig. 5c). In addition, the combination of SiO_3^{2-} and Zn^{2+} indeed revealed a synergistic effect on HHDPCs and significantly promoted cell migration and viability as compared with the Zn^{2+} or SiO_3^{2-} alone. In terms of gene expression, it is interesting that SiO_3^{2-} alone does not effectively promote the expression of stem cell indicator markers (VEGF, HGF, BMP-6, KGF), while Zn^{2+} alone stimulated VEGF and BMP-6 expression. In contrast, when the two are combined, the expression of all four genes were stimulated. It seems that Zn^{2+} are mainly responsible for hair follicle specific activation, while SiO_3^{2-} are more general activators to further enhance the specific activation by Zn^{2+}. Previous studies have shown that Zn^{2+} are necessary cofactors for a variety of proteases (alkaline phosphatase, dopachrome tautomerase, metallothionein, and metalloproteinase) [22–26]. These protease is expressed specifically in the HHDPCs of anagen hair follicles and is suggested to be one of the modulators of the cyclic growth of hair follicles [22,24,53]. Therefore, when Zn^{2+} activate the proteases in HHDPCs, the cell viability of HHDPCs increases [53–55], and HHDPCs might reach a basic conditions for differentiation. But, the activation of Zn^{2+} alone may not be strong enough. SiO_3^{2-} have been found to stimulate cellular behaviors, and in general they do not stimulate cell differentiation without addition of other differentiation inducers. Previous studies have shown that SiO_3^{2-} only enhance the proliferation and stemness maintenance of bone marrow mesenchymal stem cells and do not affect cell differentiation when they are culturing without differentiation inducer. However, when the cells are cultured with the inducer for adipogenic differentiation, the addition of SiO_3^{2-} significantly enhances the adipogenic differentiation of stem cells [39]. Here we observed similar phenomenon with HHDPCs, and found that the SiO_3^{2-} only activated some cell activity such as cell migration, but did not affect cell differentiation, while Zn^{2+} activated cell differentiation at a low level. The synergistic activity of Zn^{2+} and SiO_3^{2-} ions in stimulating hair follicle growth was further confirmed by ex vivo culture of human hair follicles. We found that the combined stimulation of Zn^{2+} and SiO_3^{2-} stimulated the growth of hair follicles in the ex vivo culture, while the Zn^{2+} and SiO_3^{2-} alone did not show stimulatory effect on hair follicle growth (Fig. S8). Our results suggest that the combination of two type of ions is critical, which act synergistically to stimulate all cellular activities including cell differentiation and hair follicle growth, and the combination of different functional ions is an effective approach to achieve highest cell activation for hair follicle regeneration and burn wound healing.

In severe skin burn, both epidermis and dermis are extensively destroyed, and the healing process is very slow [51,56]. In our previous research, it has been found that SiO_3^{2-} can effectively promote normal skin wound healing by stimulating angiogenesis [31–35]. However, epithelial regeneration after deep skin burns is critical for the healing [56], and it is not clear whether SiO_3^{2-} alone can stimulate the repair of the epithelial layer, although we have previously found that the bioceramic extract of the Si–Mg system promotes epithelial repair [57]. In the present study, we found that SiO_3^{2-} alone does not significantly promote epithelial regeneration. The wound treated with CS-SWD did not show obvious new epithelial tissue formation after the 24th day, and the wound healing rate was not significantly different from that of the Blank group. However, the ZnCS-SWD group showed a significant effect on skin epithelial regeneration, and the formation of a new epidermal layer was clearly observed (Fig. 3d), indicating that the combination of Zn^{2+} and SiO_3^{2-} can synergistically promote epithelial regeneration. We know that in the process of wound healing, in addition to fibroblasts, endothelial cells and other cells, hair follicle stem cells also participate in the process of skin epithelial regeneration [58–60], and hair follicle stem cells can be recruited and differentiated to form epithelial tissue and vascular tissue by bioactive stimuli [58,61], and the combination of Zn^{2+} and SiO_3^{2-} is likely to play a bioactive role in activating, recruiting, and inducing differentiation of hair follicle stem cells. We found that after ZnCS-SWD treatment, strong K19 positive staining was observed in the epidermis layer (Fig. S4), suggesting that the Zn–Si composite dressing may have the activity to recruit hair follicle stem cells to the epidermis area. In addition, we also found that, as compared with other groups, the expression of angiogenic growth factor VEGF in HHDPCs cultured in the presence of Zn^{2+} and SiO_3^{2-} was also significantly increased (Fig. 5d), which indicates the possible contribution of hair follicle-related cells to angiogenesis [61,62]. The results of CD31 immunohistochemical staining in animal experiments also confirmed that the ZnCS-SWD group had more blood vessel formation as compared with other groups (Fig. 4c). These results suggest that the synergistic effect of Zn^{2+} and SiO_3^{2-} released from ZnCS-SWD can effectively activate hair follicle cells to participate in the re-epithelialization and blood vessel formation of burned skin, while SiO_3^{2-} alone do not contribute much to re-epithelialization [63,64].

5. Conclusions

Large amounts of wound exudates and hair follicle regeneration are two critical problems related to burn wound healing. Our dressing design is focusing on these two problems and have function in both absorbing wound exudates and enhancing hair follicle growth. In this study, we constructed an organic-inorganic Janus membrane by wrapping hydrophilic ZnCS ceramic particles with hydrophobic PLA fiber membrane. This sandwich-structured wound dressing effectively absorbed wound exudates from wound bed and meanwhile released Zn^{2+} and SiO_3^{2-} bioactive ions into wound bed to promote rapid healing with hair follicle regeneration. The biological activity of the wound dressing is mainly due to the synergistic effect of Zn^{2+} and SiO_3^{2-}, which effectively stimulated the migration, viability and differentiation of cultured hair follicle dermal papilla cells, and in vivo results further revealed that this synergistic activity also resulted in the recruitment of hair follicle stem cells and enhancement of epidermis formation. Our study suggests that a hydrophilic inorganic layer combined with a hydrophobic organic layer can also construct a Janus membrane with unidirectional fluid transportation ability, and combination of different type of functional ions may have synergistic bioactivity to further stimulation of burn wound healing with enhanced epidermis formation and regeneration of skin appendages such as hair follicles.

Data availability statement

The raw/processed data forms part of an ongoing study and may be requested from the authors.

Author contributions statement

Z. Zhang drawn up the plan, carried on the experiments, analyzed experimental data and wrote this manuscript. Dr. F. Guo, B. Li, L. Ma, H. Zhuang & E. Wang, performed animal experiments and participated in data analysis. Y. Liu and Dr. Z. Yang cultured human hair follicle organs in ex vivo. Prof. J. Chang, Prof. C. Wu & Prof. Z. Huan discussed the data. Prof. J. Chang initiated, designed, and supervised the study, and revised this manuscript.

Declaration of competing interest

There are no conflicts of interest in this work.

Acknowledgements

This work was supported by the National Key Research and Development Program of China (No. 2016YFC1100201), the National Natural Science Foundation of China (No. 81772078), the National Natural Science Foundation of China (No. 81671830) and the Science and Technology Commission of Shanghai Municipality (No. 19441902300).

Appendix A. Supplementary data

Supplementary data to this article can be found online at https://doi.org/10.1016/j.bioactmat.2020.12.006.

References

[1] K. Lay, T. Kume, E. Fuchs, FOXC1 maintains the hair follicle stem cell niche and governs stem cell quiescence to preserve long-term tissue-regenerating potential, Proc. Natl. Acad. Sci. U.S.A. 113 (11) (2016) E1506–E1515.
[2] M. Ohyama, Hair follicle bulge: a fascinating reservoir of epithelial stem cells, J. Dermatol. Sci. 46 (2) (2007) 81–89.
[3] S.A. Castleberry, A. Golberg, M. Abu Sharkh, S. Khan, B.D. Almquist, W.G. Austen, M.L. Yarmush, P.T. Hammond, Nanolayered siRNA delivery platforms for local silencing of CTGF reduce cutaneous scar contraction in third-degree burns, Biomaterials 95 (2016) 22–34.
[4] H.E. Abaci, A. Coffman, Y. Doucet, J. Chen, J. Jackow, E. Wang, Z.Y. Guo, J. U. Shin, C.A. Jahoda, A.M. Christiano, Tissue engineering of human hair follicles using a biomimetic developmental approach, Nat. Commun. 9 (2018) 11.
[5] M. Ito, G. Cotsarelis, Is the hair follicle necessary for normal wound healing? J. Invest. Dermatol. 128 (5) (2008) 1059–1061.
[6] S. Hettiaratchy, R. Papini, ABC of burns - initial management of a major burn: II - assessment and resuscitation, Br. Med. J. 329 (7457) (2004) 101–103.
[7] M. Madaghiele, C. Demitri, A. Sannino, L. Ambrosio, Polymeric hydrogels for burn wound care: advanced skin wound dressings and regenerative templates, Burns Trauma 2 (4) (2014) 153–161.
[8] L. Shi, X. Liu, W. Wang, L. Jiang, S. Wang, A self-pumping dressing for draining excessive biofluid around wounds, Adv. Mater. 31 (5) (2019).
[9] J. Stojkovska, Z. Djurdjevic, I. Jancic, B. Bufan, M. Milenkovic, R. Jankovic, V. Miskovic-Stankovic, B. Obradovic, Comparative in vivo evaluation of novel formulations based on alginate and silver nanoparticles for wound treatments, J. Biomater. Appl. 32 (9) (2018) 1197–1211.
[10] R. Tian, X.Y. Qin, P.Y. Yuan, K. Lei, L. Wang, Y.K. Bai, S.Y. Liu, X. Chen, Fabrication of self-healing hydrogels with on-demand antimicrobial activity and sustained biomolecule release for infected skin regeneration, ACS Appl. Mater. Interfaces 10 (20) (2018) 17018–17027.
[11] H. Li, A. Granados, E. Fernandez, R. Pleixats, A. Vallribera, Anti-inflammatory cotton fabrics and silica nanoparticles with potential topical medical applications, ACS Appl. Mater. Interfaces 12 (23) (2020) 25658–25675.
[12] I. Cruz-Maya, V. Guarino, A. Almaguer-Flores, M.A. Alvarez-Perez, A. Varesano, C. Vineis, Highly polydisperse keratin rich nanofibers: scaffold design and in vitro characterization, J. Biomed. Mater. Res. A 107 (8) (2019) 1803–1813.
[13] T. Guo, X. Yang, J. Deng, L. Zhu, B. Wang, S. Hao, Keratin nanoparticles-coating electrospun PVA nanofibers for potential neural tissue applications, J. Mater. Sci. Mater. Med. 30 (1) (2019).
[14] V. Jesumani, H. Du, M. Aslam, P.B. Pei, N. Huang, Potential use of seaweed bioactive compounds in skincare-A review, Mar. Drugs 17 (12) (2019) 19.
[15] J.I. Kang, S.C. Kim, S.C. Han, H.J. Hong, Y.J. Jeon, B. Kim, Y.S. Koh, E.S. Yoo, H. K. Kang, Hair-loss preventing effect of grateloupia elliptica, Biomol. Ther. 20 (1) (2012) 118–124.
[16] F. Ayaz, E. Eker-Develi, M. Sahin, First report of Nitzschia navis-varingica in the Mediterranean Sea and growth stimulatory effects of Nitzschia navis-varingica, Chrysochromulina alifera and Heterocapsa pygmaea on different mammalian cell types, Mol. Biol. Rep. 45 (4) (2018) 571–579.
[17] Y.R. Lee, S. Bae, J.Y. Kim, J. Lee, D.H. Cho, H.S. Kim, I.S. An, S. An, Monoterpenoid loliolide regulates hair follicle inductivity of human dermal papilla cells by activating the AKT/beta-Catenin signaling pathway, J. Microbiol. Biotechnol. 29 (11) (2019) 1830–1840.
[18] J. Peng, J.P. Yuan, C.F. Wu, J.H. Wang, Fucoxanthin, a marine carotenoid present in Brown seaweeds and diatoms: metabolism and bioactivities relevant to human health, Mar. Drugs 9 (10) (2011) 1806–1828.
[19] J.N. Audinot, C. Guignard, H.N. Migeon, L. Hoffmann, Study of the mechanism of diatom cell division by means of Si-29 isotope tracing, Appl. Surf. Sci. 252 (19) (2006) 6813–6815.
[20] A. Ibuot, A.P. Dean, J.K. Pittman, Multi-genomic analysis of the cation diffusion facilitator transporters from algae, Metallomics 12 (4) (2020) 617–630.
[21] P. Yuan, D. Liu, J.M. Zhou, Q. Tian, Y.R. Song, H.H. Wei, S. Wang, J.Y. Zhou, L. L. Deng, P.X. Du, Identification of the occurrence of minor elements in the structure of diatomaceous opal using FIB and TEM-EDS, Am. Mineral. 104 (9) (2019) 1323–1335.
[22] B.K. Handjiski, S. Eichmuller, U. Hofmann, B.M. Czarnetzki, R. Paus, Alkaline-phosphatase activity and localization during the murine hair cycle, Br. J. Dermatol. 131 (3) (1994) 303–310.
[23] V.R. Martinez, M.V. Aguirre, J.S. Todaro, O.E. Piro, G.A. Echeverria, L.G. Naso, E. G. Ferrer, P.A.M. Williams, Interaction of Zn with losartan. Activation of intrinsic apoptotic signaling pathway in lung cancer cells and effects on alkaline and acid phosphatases, Biol. Trace Elem. Res. 186 (2) (2018) 413–429.
[24] P.M. Plonka, B. Handjiski, D. Michalczyk, M. Popik, R. Paus, Oral zinc sulphate causes murine hair hypopigmentation and is a potent inhibitor of eumelanogenesis in vivo, Br. J. Dermatol. 155 (1) (2006) 39–49.
[25] H.F. Guo, G.H. Cui, R. Khan, H.X. Jia, J.X. Zhang, S.H.A. Raza, M. Ayaz, M. Shafiq, L. Zan, Molecular structure and functions of zinc binding metallothionein-1 protein in mammalian body system, Pak. J. Pharm. Sci. 33 (4) (2020) 1719–1726.
[26] B. Chakrabarti, H.R. Bairagya, B.P. Mukhopadhyay, K. Sekar, New biochemical insight of conserved water molecules at catalytic and structural Zn2+ ions in human matrix metalloproteinase-I: a study by MD-simulation, J. Mol. Model. 23 (2) (2017) 13.
[27] P.M. Plonka, B. Handjiski, M. Popik, D. Michalczyk, R. Paus, Zinc as an ambivalent but potent modulator of murine hair growth in vivo - preliminary observations, Exp. Dermatol. 14 (11) (2005) 844–853.
[28] M.S. Kil, C.W. Kim, S.S. Kim, Analysis of serum zinc and copper concentrations in hair loss, Ann. Dermatol. 25 (4) (2013) 405–409.
[29] T. Karashima, D. Tsuruta, T. Hamada, F. Ono, N. Ishii, T. Abe, B. Ohyama, T. Nakama, T. Dainichi, T. Hashimoto, Oral zinc therapy for zinc deficiency-related telogen effluvium, Dermatol. Ther. 25 (2) (2012) 210–213.
[30] Y. Zhang, M. Chang, F. Bao, M. Xing, E. Wang, Q. Xu, Z. Huan, F. Guo, J. Chang, Multifunctional Zn doped hollow mesoporous silica/polycaprolactone electrospun membranes with enhanced hair follicle regeneration and antibacterial activity for wound healing, Nanoscale 11 (13) (2019) 6315–6333.
[31] Q.Y. Zeng, Y. Han, H.Y. Li, J. Chang, Design of a thermosensitive bioglass/agarose-alginate composite hydrogel for chronic wound healing, J. Mat. Chem. B 3 (45) (2015) 8856–8864.
[32] H.Y. Li, J. He, H.F. Yu, C.R. Green, J. Chang, Bioglass promotes wound healing by affecting gap junction connexin 43 mediated endothelial cell behavior, Biomaterials 84 (2016) 64–75.
[33] H.F. Yu, J.L. Peng, Y.H. Xu, J. Chang, H.Y. Li, Bioglass activated skin tissue engineering constructs for wound healing, ACS Appl. Mater. Interfaces 8 (1) (2016) 703–715.
[34] X. Dong, J. Chang, H.Y. Li, Bioglass promotes wound healing through modulating the paracrine effects between macrophages and repairing cells, J. Mat. Chem. B 5 (26) (2017) 5240–5250.
[35] Y.L. Zhang, X. Niu, X. Dong, Y. Wang, H.Y. Li, Bioglass enhanced wound healing ability of urine-derived stem cells through promoting paracrine effects between stem cells and recipient cells, J. Tissue Eng. Regen. Med. 12 (3) (2018) E1609–E1622.
[36] H. Ma, Q. Zhou, J. Chang, C. Wu, Grape seed-inspired smart hydrogel scaffolds for melanoma therapy and wound healing, ACS Nano 13 (4) (2019) 4302–4311.
[37] M. Yi, H. Li, X. Wong, J. Yan, L. Gao, Y. He, X. Zhong, Y. Cai, W. Feng, Z. Wen, C. Wu, C. Ou, J. Chang, M. Chen, Ion therapy: a novel strategy for acute myocardial infarction, Adv. Sci. 6 (1) (2019).
[38] Y. Zhou, C. Wu, J. Chang, Bioceramics to regulate stem cells and their microenvironment for tissue regeneration, Mater. Today 24 (2019) 41–56.
[39] X. Wang, L. Gao, Y. Han, M. Xing, C. Zhao, J. Peng, J. Chang, Silicon-enhanced adipogenesis and angiogenesis for vascularized adipose tissue engineering, Adv. Sci. 5 (11) (2018).
[40] T. Tian, Y. Han, B. Ma, C.T. Wu, J. Chang, Novel Co-akermanite (Ca2CoSi2O7) bioceramics with the activity to stimulate osteogenesis and angiogenesis, J. Mat. Chem. B 3 (33) (2015) 6773–6782.
[41] X.T. Wang, L.Y. Wang, Q. Wu, F. Bao, H.T. Yang, X.Z. Qiu, J. Chang, Chitosan/calcium silicate cardiac patch stimulates cardiomyocyte activity and myocardial performance after infarction by synergistic effect of bioactive ions and aligned nanostructure, ACS Appl. Mater. Interfaces 11 (1) (2019) 1449–1468.
[42] T. Tian, C.T. Wu, J. Chang, Preparation and in vitro osteogenic, angiogenic and antibacterial properties of cuprorivaite (CaCuSi4O10, Cup) bioceramics, RSC Adv. 6 (51) (2016) 45840–45849.
[43] A. Abdal-Hay, A. Memic, K.H. Hussein, Y.S. Oh, M. Fouad, F.F. Al-Jassir, H. M. Woo, Y. Morsi, X.M. Mo, S. Ivanovski, Rapid fabrication of highly porous and biocompatible composite textile tubular scaffold for vascular tissue engineering, Eur. Polym. J. 96 (2017) 27–43.
[44] Z.W.B. Zhang, Q.X. Dai, Y. Zhang, H. Zhuang, E.D. Wang, Q. Xu, L.L. Ma, C.T. Wu, Z.G. Huan, F. Guo, J. Chang, Design of a multifunctional biomaterial inspired by ancient Chinese medicine for hair regeneration in burned skin, ACS Appl. Mater. Interfaces 12 (11) (2020) 12489–12499.
[45] Y. Zhang, M.L. Chang, F. Bao, M. Xing, E. Wang, Q. Xu, Z.G. Huan, F. Guo, J. Chang, Multifunctional Zn doped hollow mesoporous silica/polycaprolactone electrospun membranes with enhanced hair follicle regeneration and antibacterial activity for wound healing, Nanoscale 11 (13) (2019) 6315–6333.
[46] R.L. Rajendran, P. Gangadaran, S.S. Bak, J.M. Oh, S. Kalimuthu, H.W. Lee, S. H. Baek, L. Zhu, Y.K. Sung, S.Y. Jeong, S.W. Lee, J. Lee, B.C. Ahn, Extracellular vesicles derived from MSCs activates dermal papilla cell in vitro and promotes hair follicle conversion from telogen to anagen in mice, Sci. Rep. 7 (2017) 12.
[47] S.M.Y. Fan, C.F. Tsai, C.M. Yen, M.H. Lin, W.H. Wang, C.C. Chan, C.L. Chen, K.K. L. Phua, S.H. Pan, M.V. Plikus, S.L. Yu, Y.J. Chen, S.J. Lin, Inducing hair follicle neogenesis with secreted proteins enriched in embryonic skin, Biomaterials 167 (2018) 121–131.
[48] H. Kamp, C.C. Geilen, C. Sommer, U. Blume-Peytavi, Regulation of PDGF and PDGF receptor in cultured dermal papilla cells and follicular keratinocytes of the human hair follicle, Exp. Dermatol. 12 (5) (2003) 662–672.

[49] L. Dong, H.J. Hao, J.J. Liu, D.D. Ti, C. Tong, Q. Hou, M.R. Li, J.X. Zheng, G. Liu, X. B. Fu, W.D. Han, A conditioned medium of umbilical cord mesenchymal stem cells overexpressing Wnt7a promotes wound repair and regeneration of hair follicles in mice, Stem Cell. Int. 2017 (2017) 13.
[50] M. Choi, S.J. Choi, S. Jang, H.I. Choi, B.M. Kang, S.T. Hwang, O. Kwon, Shikimic acid, a mannose bioisostere, promotes hair growth with the induction of anagen hair cycle, Sci. Rep. 9 (2019) 8.
[51] A. Shpichka, D. Butnaru, E.A. Bezrukov, R.B. Sukhanov, A. Atala, V. Burdukovskii, Y.Y. Zhang, P. Timashev, Skin tissue regeneration for burn injury, Stem Cell Res. Ther. 10 (2019) 16.
[52] L. Gao, Y. Zhou, J. Peng, C. Xu, Q. Xu, M. Xing, J. Chang, A novel dual-adhesive and bioactive hydrogel activated by bioglass for wound healing, NPG Asia Mater. 11 (2019).
[53] T. Anan, T. Sonoda, Y. Asada, S. Kurata, S. Takayasu, Protease-activated receptor-1 (thrombin receptor) is expressed in mesenchymal portions of human hair follicle, J. Invest. Dermatol. 121 (4) (2003) 669–673.
[54] Y. Si, J.B. Zhang, J.Z. Bai, Q. Li, Y. Mo, J. Wu, R.H. Fang, Effects of cathepsin B on proliferation, activation, and melanin synthesis of human hair follicle melanocytes, Int. J. Clin. Exp. Med. 11 (8) (2018) 8170–8175.
[55] T. Reinheckel, S. Hagemann, S. Dollwet-Mack, E. Martinez, T. Lohmuller, G. Zlatkovic, D.J. Tobin, N. Maas-Szabowski, C. Peters, The lysosomal cysteine protease cathepsin L regulates keratinocyte proliferation by control of growth factor recycling, J. Cell Sci. 118 (15) (2005) 3387–3395.
[56] Y. Wang, J. Beekman, J. Hew, S. Jackson, A.C. Issler-Fisher, R. Parungao, S. S. Lajevardi, Z. Li, P.K.M. Maitz, Burn injury: challenges and advances in burn wound healing, infection, pain and scarring, Adv. Drug Deliv. Rev. 123 (2018) 3–17.
[57] F. Wang, X. Wang, K. Ma, C. Zhang, J. Chang, X. Fu, Akermanite bioceramic enhances wound healing with accelerated reepithelialization by promoting proliferation, migration, and stemness of epidermal cells, Wound Repair Regen.Off. Publ. Wound Healing Soc. Eur. Tissue Repair Soc. 28 (1) (2020) 16–25.
[58] K.A.U. Gonzales, E. Fuchs, Skin and its regenerative powers: an alliance between stem cells and their niche, Dev. Cell 43 (4) (2017) 387–401.
[59] B.M. Li, W.Z. Hu, K. Ma, C.P. Zhang, X.B. Fu, Are hair follicle stem cells promising candidates for wound healing? Expet Opin. Biol. Ther. 19 (2) (2019) 119–128.
[60] Y. Han, Y.H. Li, Q.Y. Zeng, H.Y. Li, J.L. Peng, Y.H. Xu, J. Chang, Injectable bioactive akermanite/alginate composite hydrogels for in situ skin tissue engineering, J. Mat. Chem. B 5 (18) (2017) 3315–3326.
[61] Z.C. Xu, Q. Zhang, H. Li, Differentiation of human hair follicle stem cells into endothelial cells induced by vascular endothelial and basic fibroblast growth factors, Mol. Med. Rep. 9 (1) (2014) 204–210.
[62] R.F. Quan, W.B. Du, X. Zheng, S.C. Xu, Q. Li, X. Ji, X.M. Wu, R.X. Shao, D.S. Yang, VEGF165 induces differentiation of hair follicle stem cells into endothelial cells and plays a role in in vivo angiogenesis, J. Cell Mol. Med. 21 (8) (2017) 1593–1604.
[63] H.Y. Li, K. Xue, N. Kong, K. Liu, J. Chang, Silicate bioceramics enhanced vascularization and osteogenesis through stimulating interactions between endothelia cells and bone marrow stromal cells, Biomaterials 35 (12) (2014) 3803–3818.
[64] B.M. Li, X.W. Bian, W.Z. Hu, X.Y. Wang, Q.K. Li, F.F. Wang, M.L. Sun, K. Ma, C. P. Zhang, J. Chang, X.B. Fu, Regenerative and protective effects of calcium silicate on senescent fibroblasts induced by high glucose, Wound Repair Regen. 28 (3) (2020) 315–325.